LM-03K116
June 9, 2003

# Self-Organized Superlattices in GaInAsSb Grown on Vicinal Substrates

C.A. Wang, C.J. Vineis and D.R. Calawa

## NOTICE

2003 MRS Fall Meeting, Boston, MA, 1-5 December 2003
Symposium T: Self-Organized Processes in Semiconductor Heteroepitaxy, Invited paper

# Self-Organized Superlattices in GaInAsSb Grown on Vicinal Substrates*

C.A. Wang, C.J. Vineis†, and D.R. Calawa
Lincoln Laboratory, Massachusetts Institute of Technology, Lexington, MA 02420-9108
†now at AmberWave Systems Corporation, Salem, NH 03079

## ABSTRACT

Self-organized superlattices are observed in GaInAsSb epilayers grown lattice matched to vicinal GaSb substrates. The natural superlattice (NSL) is oriented at a slight angle of about 4° with respect to the vicinal (001) GaSb substrate. This vertical composition modulation is detected at the onset of growth. Layers in the NSL are continuous over the lateral extent of the substrate. Furthermore, the NSL persists throughout several microns of deposition. The NSLs have a period ranging from 10 to 30 nm, which is dependent on deposition temperature and GaInAsSb alloy composition. While the principle driving force for this type of phase separation is chemical, the mechanism for the self-organized microstructure is related to local strains associated with surface undulations. By using a substrate with surface undulations, the tilted NSL can be induced in layers with alloy compositions that normally do not exhibit this self-organized microstructure under typical growth conditions. These results underscore the complex interactions between compositional and morphological perturbations.

## INTRODUCTION

Phase separation in multi-component compound semiconductors has been widely reported [1]. Of particular interest are materials systems that spontaneously self-organize with a significant degree of regularity, since this periodicity can impact the electronic band structure and consequently, materials properties and device performance. The length scale of these ordered phases ranges from the atomic scale, e.g. CuPt ordering as observed in GaInP [2], GaAsP [3], GaAsSb, [4], and InAsSb [5], to microscopic dimensions on the order of ~50 nm, e.g. composition modulation. Composition modulation can persist either parallel (lateral) to the growth direction, or perpendicular (vertical) to the growth direction. Lateral composition modulation (LCM) has been reported in strained alloy systems such as bulk AlInAs and GaInP epilayers [6-8], as well as in short period superlattices such as GaP/InP, AlAs/InAs, GaAs/InAs, and InAs/GaSb [9-12].

Vertical composition modulation (VCM) and self-organized natural superlattices (NSLs) in alloy layers that are homogenously grown have also been observed, but these studies are less prevalent and the mechanism for their formation are less understood. NSLs have been reported in ZnSeTe grown on vicinal GaAs substrates [13] and SiGe grown on (001) Si [14]. The NSL period was 2 to 3 nm for both of these materials systems, and a model based on step-flow growth and local strain fields that are modulated during growth were developed to explain the phenomena [14]. In addition, InAsSb and GaAsSb [5,15] were reported to spontaneously form a periodic structure that consisted of platelets of alternating composition and periodicity on the order of 20 to 50 nm. Both InAsSb and GaAsSb exhibit miscibility gaps [16], and this larger scale modulation was attributed to the tendency for these alloys to phase separate. It was speculated that islands of the different phases develop at the growth surface and then

*This work was sponsored by the Department of Energy under AF Contract No. F19628-00-C-0002. The opinions, interpretations, conclusions and recommendations are those of the author and are not necessarily endorsed by the United States Government.

subsequently laterally overgrow each other. While atomic ordering and VCM were simultaneously observed in InAsSb and GaAsSb [5], VCM without ordering was reported for GaInP [17]. In that study, the alloy was also grown on a vicinal substrate, and dark and light bands parallel to the growth surface were observed in cross-section transmission electron microscopy (TEM). The periodicity of the VCM was 10 to 12 nm. More recently, spontaneous superlattice formation was observed for GaInAsSb [18], AlGaInN [19] and AlGaInAsSb [20]. The NSLs have modulation period ranging 10 to 30 nm. It is interesting to note, however, that Ref. 20 also reported that no NSLs were observed in either GaInAsSb or AlGaAsSb.

The common thread in these reports on VCM is that each of the alloys studied exhibits a miscibility gap, and epilayers were grown below the critical temperature for phase separation [16]. In fact, the spinodal-like contrast in TEM [1], which is a common manifestation of phase-separated alloys, can also be present. However, the periodicity associated with VCM is less frequently reported, and the mechanism for the self-organization is unclear. This work reports spontaneous formation of self-organized NLSs in GaInAsSb alloys grown nominally lattice matched to vicinal GaSb substrates. The NSL is tilted 4° with respect to the substrate miscut angle, and the NSL period is correlated with the wavelength of surface undulations on the epilayer. Furthermore, as the In and As composition is increased, which drives the alloy further into the miscibility gap, both the intensity of the NLS and amplitude of surface undulations increase.

## EXPERIMENTAL APPROACH

GaInAsSb epitaxial layers were grown nominally lattice matched to (001) GaSb substrates with miscut angles of 2 or 6° toward (-1-11)A, (1-11)B, or (101) by OMVPE as previously described [21,22]. The growth temperature ranged from 525 to 575 °C. Trimethylindium, triethylgallium, tertiarybutylarsine, and trimethylantimony were used as organometallic precursors. Growth was initiated by simultaneously flowing the four precursors into the OMVPE reactor. The growth rate was ~5 μm/hr, and the layers were typically 1 to 4 μm in thickness. The GaInAsSb alloy composition was determined from the peak energy in 300 K photoluminescence (PL) spectra and lattice mismatch as measured by high-resolution x-ray diffraction (HRXRD) [21]. In addition, the full-width at half-maximum of PL spectra at 4K were used to assess alloy non-uniformity [23].

Several methods were used to characterize the CM and NSL. The microstructure of GaInAsSb was studied by examining <1-10> and <110> cross-sections in field-emission scanning electron microscopy (FE-SEM) and TEM operated at 200 kV. For TEM, the NSL was imaged using g = <222> or <111> 2-beam conditions, in either bright- or dark-field conditions. In addition, HRXRD rocking curves and reciprocal space x-ray maps (RSXRM) were used to quantitatively determine the angle of lattice tilt and period of the tilted NLS. The surface morphology was characterized by atomic force microscopy (AFM) operating in tapping mode, and was used to correlate the microstructure with the surface undulations.

## RESULTS

Bright-field (BF) <110> cross-section TEM images of GaInAsSb layers grown at 525 °C on (001) GaSb substrates miscut 6° toward (1-11)B are shown in Fig. 1. $Ga_{0.89}In_{0.11}As_{0.09}Sb_{0.91}$ in Fig. 1a has a 300 K PL peak at 2.09 μm, while $Ga_{0.8}In_{0.2}As_{0.17}Sb_{0.83}$ in Fig. 1b has a peak at 2.485 μm. The higher InAs content increases the PL peak energy and corresponds to an alloy that penetrates further into the miscibility gap. Minimal TEM diffraction contrast is observed for the GaInAsSb epilayer with shorter PL peak wavelength (Fig. 1a), while significant spinodal-like contrast [1] is observed for GaInAsSb epilayer with longer PL peak wavelength (Fig. 1b). This contrast results from the strain that is associated with phase separation into GaAs- and InSb-rich regions [24,25]. The 4 K PL FWHM of these samples was 4.3 and 9.5 meV, respectively for Fig. 1a and 1b, respectively. The value for the sample in Fig. 1b is considerably small despite the inhomogeneity of the microstructure.

In addition to the spinodal-like contrast observed in the sample shown in Fig. 1b, a self-organized NLS was observed. Figure 2 shows a [110] cross-section TEM image illustrating the NLS. The image was obtained using a dark-field (DF) <222> 2-beam condition. The NLS has a 10° tilt with respect to the surface normal, which is an additional 4° compared to the 6° miscut angle. The NSL is observed at the onset of growth; is laterally continuous throughout the epilayer; and maintains a consistent periodicity of 20 nm throughout the 2-μm-thick epilayer.

This tilted NSL could also be imaged in FE-SEM, as shown in Fig. 3. Figures 3a and 3b show [-1-10] and [1-10] cross-section FE-SEM images of the sample shown in Fig. 1(b). The sample received a brief stain etch before imaging in the FE-SEM. The tilted superlattice is clearly observed throughout the epilayer, with a period of 20 nm and a tilt angle of 10° with respect to the surface normal (Fig. 3a). These results are consistent with the TEM image shown in Fig. 2. The orthogonal cross-section (Fig. 3b) shows a parallel superlattice. A schematic of the geometry of the microstructure is shown in Fig. 4.

The tilted NSL can also be characterized by RSXRM. Figures 5a and 5b show a HRXRD rocking curve and RSXRM, respectively, of $Ga_{0.8}In_{0.2}As_{0.17}Sb_{0.83}$. Satellite peaks that are observed in the HRXRD are symmetric about the epilayers peak. Lattice tilt is clearly seen in the reciprocal space map, and the tilt angle can be quantitatively measured. It was determined to be 9.7°, which is consistent with the TEM and FE-SEM characterization.

These results show that a variety of techniques including TEM, FE-SEM, and HRXRD can be used to characterize the tilted NSL, and additional samples grown under various conditions were characterized using one or more of the above methods. The effect of substrate misorientation angle was investigated for GaInAsSb grown on (001) GaSb miscut either 2, 4,or 6° toward [1-11]B. Using RSXRM, the tilt angle of the NSL was measured to be 6.3, 8.1, and 9.6° with respect to the substrate normal for the 2, 4, and 6° miscut substrates, respectively. These results indicate that the tilted microstructure maintains a 4° tilt with respect to the substrate miscut, independent of the miscut angle.

The effect on alloy composition on the intensity of the tilted microstructure was determined by RSXRM, and Figure 6 shows these maps for three different alloy compositions grown on (001) GaSb miscut 6° toward [1-10]. The 300 K PL peak wavelengths from the samples are 2.09, 2.07, and 2.485 μm for Figs. 6a, 6b, and 6c, respectively. The intensity associated with the tilted microstructure increases with increasing PL peak wavelength, i.e., as the alloy composition moves further into the miscibility gap.

AFM images of the morphology of GaInAsSb epilayer surfaces are shown in Figure 7. Figure 7a is GaInAsSb grown at 525 °C on (001) GaSb miscut 6° toward [1-11]B and Fig. 7b is GaInAsSb grown at 575 °C on (001) GaSb miscut 2° toward [101]. A surface undulation is observed for both of these images, and it is characteristic of all the samples that exhibit the tilted NLS. The surface step structure of GaInAsSb grown at 525 °C is vicinal, while it is step-bunched at 575 °C [23], and the sample shown in Fig. 7b exhibits both the step bunching and surface undulations.

The wavelength of these surface undulations is directly correlated with the period of the tilted NSL. The surface undulation of the AFM image shown in Fig. 7a has a lateral period of about 115 nm. The tilted NSL has a period of 20 nm and a tilt angle of 10°. Simple geometry indicates that when a 20 nm period tilted at a 10° angle intersects the surface, it will have a lateral period of: 20 nm / sin (10°) = 115 nm. Thus, the lateral period of the tilted NSL and the surface undulations is the same. Table I shows several examples of this correlation. Note that the period of the NSL is larger for a smaller misorientation angle. Furthermore, it was found that the amplitude of the surface undulation increases with the strength of the tilted NSL as observed in RSXRM. The amplitude of the undulation is less than 1 nm for the sample shown in Fig. 6a, while it is 4-5 nm for the sample shown in Fig. 6c.

These results suggest that the tilted NSL and surface undulations are coupled. To further test this hypothesis, a structure was specially grown. The layer structure is shown in Figure 8. It consists of different alloy compositions of GaInAsSb, separated by 2 nm GaSb. The alloy composition of layers #1 and #5 is similar to that of the layer shown in Figs. 1a and 6a, while the alloy composition of layer #3 is similar to that of the layer shown in Figs. 1b and 2. Therefore, observations of a tilted NSL and strong spinodal-like contrast are anticipated in layer #3, but not in layers #1 and #5.

Figure 9 shows the cross-section TEM images of the grown sample. As expected, the <220> image (Fig. 9a) indicates that layers #1 and #5 barely exhibit more contrast than the GaSb substrate, while layer #3 exhibits strong spinodal-like contrast. Figure 9b shows a <222> 2-beam image of the substrate, buffer layer, and layers #1-3, while Figure 9c shows layers #3-5. As expected based on results shown in Figs. 1a and 6a, no NSL is observed in layer #1, and a 10° tilted NSL is observed in layer #3 (Fig. 9b). However, a tilted NSL in layer #5 (Fig. 9c) is observed throughout the entire epilayer, although it appeared to weaken as growth proceeded.

The tilted NSL present in layer #3 was propagated into layer #5, even though the NSL was not present in layer #1 and layers #1 and 5 were grown under the same temperature and flow conditions. These images clearly illustrate the coupling of compositional and morphological perturbations [26-29]. The composition associated with layer #5 does not inherently phase

separate to form a tilted NSL, it did so in this special case because surface undulations present from layer #3 created a surface strain field that continued to drive lateral surface segregation. The lateral period of the dark and light regions in layer #4 is about 100 nm. This correlates with the tilted NSL, which had a period of 17.2 nm and a tilt angle of 9.7°, yielding a lateral period of [17.2 nm / sin (9.7°)] = 102 nm. The surface peaks continued to preferentially incorporate InSb-rich GaInAsSb, while the surface valleys preferentially incorporated GaAs-rich GaInAsSb. Therefore, the composition modulation associated with the tilted NSL is directly coupled to the surface undulations, and shows that surface strain / roughness can promote phase separation.

## DISCUSSION

These observations are in line with models developed by Venezuela et al [14], which predicted phase separation for alloys grown on surfaces with modulated strain fields. However, since that model depends on alloy decomposition at step bunches, the NSL period is only on the order of a few nm. Therefore, that model cannot fully explain the larger NSL periods observed in this study. This suggests that surface undulations are directly related to the tilted NSL. It is proposed that surface undulations play a similar role to step bunches in the Venezuela model.

A qualitative model for development of the tilted superlattice is proposed. During deposition of the first few monolayers of GaInAsSb, a random mix of Ga, In, As, and Sb adatoms is present on the surface of the GaSb substrate. Due to the thermodynamic driving force of the miscibility gap, adatoms segregate to form a lateral composition modulation, with one phase slightly enriched in InSb and another slightly enriched in GaAs. Once such lateral composition modulation forms, a large elastic strain field along the surface is generated from the lattice-mismatch between the two GaInAsSb phases enriched in GaAs and InSb. As Glas has recently shown theoretically [29], a surface with such a lateral composition modulation can effectively relieve its strain if the larger lattice constant phase (the InSb-rich phase in this case) forms peaks, while the smaller lattice constant phase (the GaAs-rich phase) forms valleys. The surface therefore forms a series of peaks and valleys, creating surface undulations, as are observed in the AFM images in Fig. 7.

Once such undulations form, all subsequent epitaxial deposition is biased so that surface peaks preferentially incorporate InSb-enriched GaInAsSb, while the surface valleys preferentially incorporate GaAs-enriched GaInAsSb. In other words, when each successive monolayer is deposited and laterally phase separates, the InSb- and GaAs-rich regions are not randomly situated with respect to the underlying InSb- and GaAs-rich regions. Rather, the new InSb- and GaAs-rich regions are strain-locked to the underlying InSb- and GaAs-rich regions due to the strain field of the surface undulations [27, 29]. This strain-locking explains the robustness of the superlattice. Such strain-locking mechanisms due to surface strain are known to play important roles in other epitaxial phenomena. One example is the vertical registry of multiple layers of quantum dots [30], while another is the atomic ordering (e.g. CuAu, CuPt) seen in many III-V ternary and quaternary compounds, which is now believed to be caused by surface reconstructions (dimers) [31].

The additional tilt of the superlattice with respect to the surface steps can be understood from a similar mechanism to that in the Venezuela model. Rather than ejection and capture of single

steps from step bunches, in this case the additional tilt is caused by ejection and capture of single steps from surface peak or valley regions. The lateral period of the undulations is typically 100-200 nm. Each peak or valley region is therefore 50-100 nm, and thus comprises on average 17-34 individual steps (for a 6° miscut) or 6-11 steps (for a 2° miscut). As epitaxial growth proceeds, if an individual step is ejected by a valley and captured by an adjacent peak, that step would switch its incorporation preference from GaAs-enrichment to InSb-enrichment. Similarly, that step would eventually be ejected from the peak and captured by the adjacent valley, switching its preference back to GaAs-enrichment. The magnitude of the additional tilt is dependent on the relative lateral velocities of the surface undulations and the individual steps that comprised those undulations.

## CONCLUSIONS

In conclusion, self-organized NSL are observed in GaInAsSb epilayers. The NSL exhibits a 4° tilt with respect to the miscut angle of the GaSb substrate, and the NSL period can be correlated with the wavelength of undulations on the epilayer surface and the substrate misorientation angle. The undulations form to relieve the local strain associated with composition modulation of the tilted NSL and demonstrates the coupling between composition modulation and morphological perturbations. A qualitative model for the propagation and robustness of the tilted NSL is discussed.

## ACKNOWLEDGMENTS

The authors gratefully acknowledge P.M. Nitishin and J.W. Chludzinski for technical assistance in materials characterization.

## REFERENCES

1. A. Zunger and S. Mahajan, Handbook of Semiconductors, edited by T.S. Moss (Elsevier Science, Amsterdam, 1994), Vol. 3, p. 1399.
2. T. Suzuki, A. Gomyo, and S. Iijima, J. Cryst. Growth 93, 396 (1988).
3. G.S. Chen, D.H. Jaw, and G.B. Stringfellow, Appl. Phys. Lett. 57, 2475 (1990).
4. H.R. Jen, M.J. Jou, Y.T. Cherng, and G.B. Stringfellow, J. Cryst. Growth 85, 175 (1987).
5. A.G. Norman, T.-Y. Seong, I.T. Ferguson, G.R. Booker, and B.A. Joyce, Semicond. Sci. Technol. 8, S9 (1993).
6. S.W. Jun, T.-Y. Seong, J.H. Lee, and B. Lee, Appl. Phys. Lett. 68, 3443 (1996).
7. B. Shin, A. Lin, K. Lappo, R.S. Goldman, M.C. Hanna, S. Francoeur, A.G. Norman, and A. Mascarenhas, Appl. Phys. Lett. 80, 3292 (2002).
8. X. Wallart, C. Priester, D. Deresmes, and F. Mollot, Appl. Phys. Lett. 77, 253 (2000).
9. K.C. Hsieh, J.N. Baillargeon, and K.Y. Cheng, Appl. Phys. Lett. 57, 2244 (1990).
10. K.Y. Cheng, K.C. Hsieh, and J.N. Baillargeon, Appl. Phys. Lett. 60, 2892 (1992).
11. C. Dorin and J. Mirecki Millunchick, J. Appl. Phys. 91, 237 (2002).
12. D.W. Stokes, R.L. Forrest, J.H. Li, S.C. Moss, B.Z. Nosho, B.R. Bennett, L.J. Whitman, and M. Goldenberg, J. Appl. Phys. 93, 311 (2003).
13. S.P. Ahrenkiel, S.H. Xin, P.M. Reimer, J.J. Berry, H. Luo, S. Short, M. Bode, M. Al-Jassim, J.R. Buschert, and J.K. Furdyna, Phys. Rev. Lett. 75, 1586 (1995).

14. P. Venezuela, J. Tersoff, J.A. Floro, E. Chason, D.M. Follstaedt, F. Liu, M.G. Lagally, Nature 397, 678 (1999).
15. I.T. Ferguson, A.G. Norman, B.A. Joyce, T.-Y. Seong, G.R. Booker, R.H. Thomas, C.C. Phillips, and R.A. Stradling, Appl. Phys. Lett. 59, 3324 (1991).
16. G.B. Stringfellow, J. Cryst. Growth 58, 194 (1982).
17. D.M. Follstaedt, R.P. Schneider, Jr., and E.D. Jones, J. Appl. Phys. 77, 3077 (1995).
18. Y.-C. Chen, V. Bucklen, K. Rajan, C.A. Wang, G.W. Charache, G. Nichols, M. Freeman, and P. Sander, Mat. Res. Soc. Symp. Proc. Vol. 583, 367 (2000).
19. N.A. El-Masry, M.K. Behbehani, S.F. LeBoeuf, M.E. Aumer, J.C. Roberts, and S.M. Bedair, Appl. Phys. Lett. 79, 1616 (2001).
20. D.H. Jaw, J.R. Chang, and Y.K. Su, Appl. Phys. Lett. 82, 3883 (2003).
21. C.A. Wang, H.K. Choi, D.C. Oakley, G.W. Charache, J. Cryst. Growth **195**, 346-355 (1998).
22. C.A. Wang, D.R. Calawa, and C.J. Vineis, J. Electron. Mater. **30**, 1392-1396 (2001).
23. C.A. Wang, Appl. Phys. Lett. 76, 2077 (2000).
24. C.A. Wang, H.K. Choi, S.L. Ransom, G.W. Charache, L.R. Danielson, and D.M. DePoy, Appl. Phys. Lett. 75, 1305 (1999).
25. P.S. Dutta and T.R. Miller, J. Electron. Mater. 29, 956 (2000).
26. J. Tersoff, Phys. Rev. B56, R4394 (1997).
27. F. Glas, J. Appl. Phys. 62, 3201 (1987).
28. F. Glas, Appl. Surf. Sci. 123/124, 298 (1998).
29. F. Glas, Phys. Rev. B 62, 7393 (2000).
30. Y.W. Zhang, S.J. Xu, C.-H. Chiu, Appl. Phys. Lett. 74, 1809 (1999).
31. L.C. Su and G.B. Stringfellow, J. Appl. Phys. 83, 3620 (1998).

| Table I. Correlation of Tilted Superlattice and Surface Undulations | | | | |
|---|---|---|---|---|
| **Miscut Angle** | **NSL Period** | **NSL Tilt Angle** | **NSL Lateral Period** | **AFM Period** |
| 6° [1-11]B | 20 nm | 10° | 115 nm | 115 nm |
| 2° [1-11]B | 14.6 nm | 5.8° | 144 nm | 143 nm |
| 2° [101] | 13.8 nm | 6.0° | 132 nm | 160 nm |

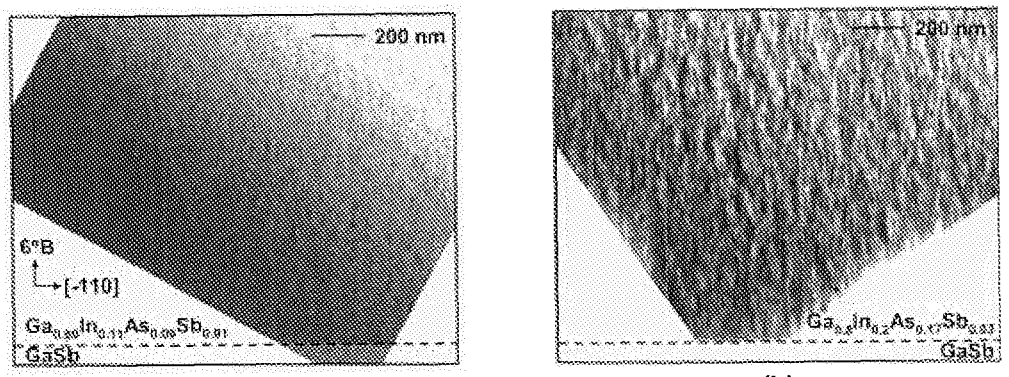


**Figure 1.** Bright field <110> cross-section TEM images using g = <220> 2-beam diffraction of GaInAsSb grown at 525 °C on substrates oriented (001) 6° toward (1-11)B: (a) $Ga_{0.89}In_{0.11}As_{0.09}Sb_{0.91}$ and (b) $Ga_{0.8}In_{0.2}As_{0.17}Sb_{0.83}$. The images are oriented so that the growth direction is straight up. The sample in (b) has a composition that was further into the miscibility gap than that in (a), and exhibits stronger spinodal-like contrast.

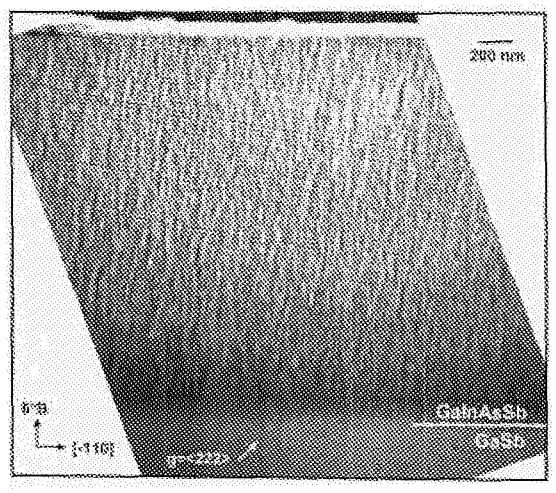


**Figure 2.** [110] Cross-section TEM image of $Ga_{0.8}In_{0.2}As_{0.17}Sb_{0.83}$ using g = <222> 2-beam conditions. Spinodal-like contrast is observed as well as a NSL. The NSL is tilted 10° from the surface normal, i.e. 4° in addition to the 6° miscut angle.

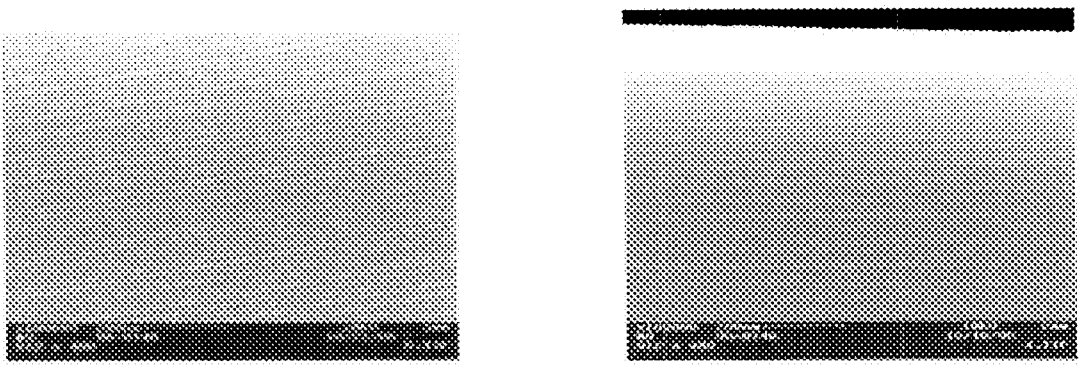


**Figure 3.** Cross-section FE-SEM images of $Ga_{0.8}In_{0.2}As_{0.17}Sb_{0.83}$ showing the NSL: (a) [-1-10] cross section and (b) [1-10] cross section.

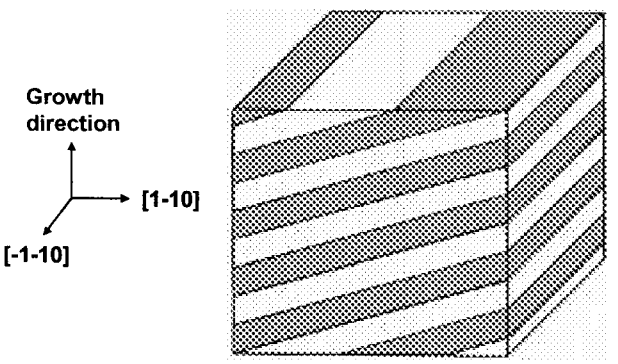


**Figure 4.** A schematic diagram of the self-organized NSL microstructure.

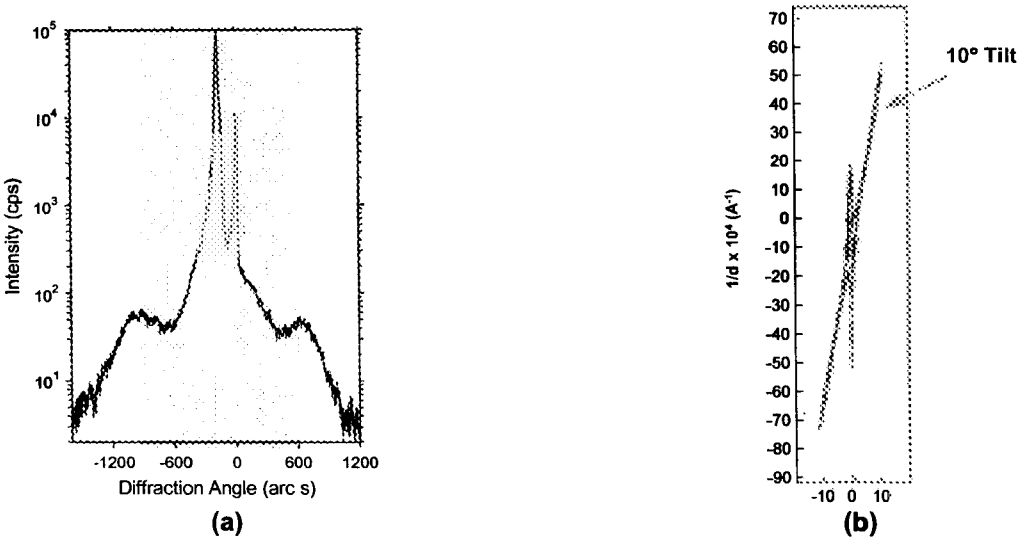


**Figure 5.** HRXRD of $Ga_{0.8}In_{0.2}As_{0.17}Sb_{0.83}$: (a) $\omega/2\theta$ scan and (b) reciprocal space map.

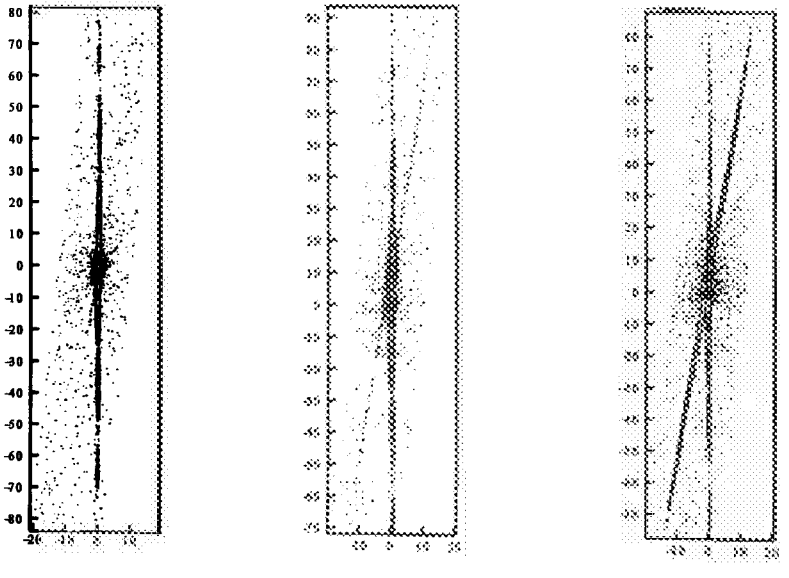


**Figure 6.** RSXRM of (a) $Ga_{0.89}In_{0.11}As_{0.09}Sb_{0.91}$, (b) $Ga_{0.85}In_{0.15}As_{0.14}Sb_{0.86}$, and (c) $Ga_{0.8}In_{0.2}As_{0.17}Sb_{0.83}$. The diffracted intensity from the tilted microstructure associated with the NSL increases with the InAs content in GaInAsSb.

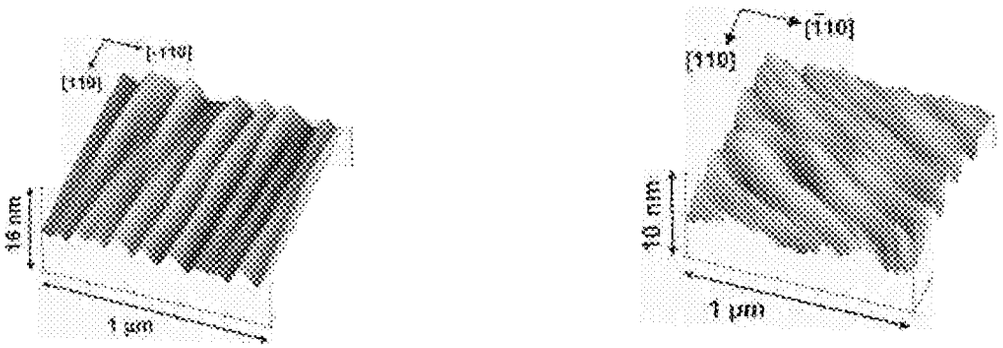


(a) (b)

**Figure 7.** AFM images of the surface undulations of GaInAsSb samples with a tilted superlattice grown on various GaSb substrate miscut orientations: (a) (001) 6 toward [1-11]B and (b) (001) toward [101].

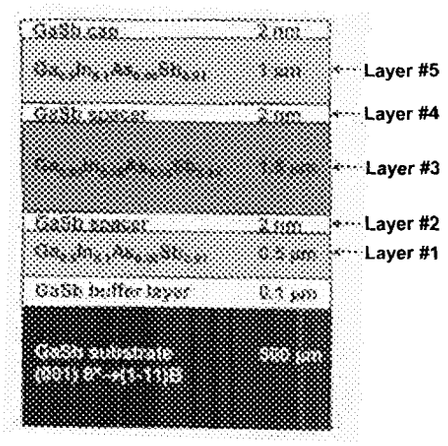


**Figure 8.** Schematic structure of specially grown GaInAsSb epitaxy to observe coupling of morphological surface undulations and compositional modulation.

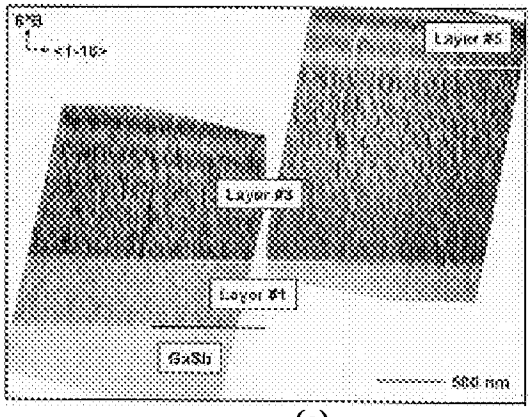


(a)

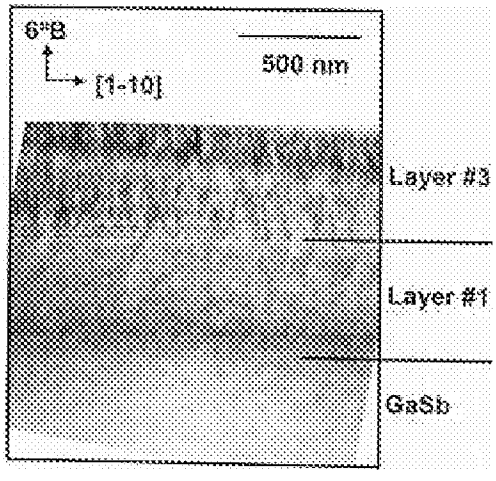


(b)

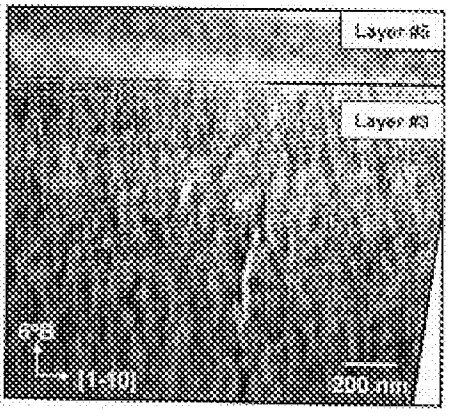


(c)

**Figure 9.** Cross-section TEM images of sample illustrated in Fig. 8: a) <220> 2-beam diffraction; b) <222> 2-beam diffraction of layers #1 - #3; (c) <222> 2-beam diffraction of layers #3 - 5.